International Journal of Applied Pharmaceutics

ISSN- 0975-7058 Vol 10, Issue 6, 2018

Original Article

CARMUSTINE LOADED LACTOFERRIN NANOPARTICLES DEMONSTRATES AN ENHANCED ANTIPROLIFERATIVE ACTIVITY AGAINST GLIOBLASTOMA *IN VITRO*

HARIKIRAN ATHMAKUR, ANAND KUMAR KONDAPI*

Department of Biotechnology and Bioinformatics, School of Life Sciences, University of Hyderabad, India
Email: akondapi@gmail.com

Received: 18 Jun 2018, Revised and Accepted: 04 Oct 2018

ABSTRACT

Objective: Despite sophisticated treatment regimens, there is no significant improvement in the mortality rates of glioblastoma due to insufficient dosage delivery, reoccurrence of tumors, higher systemic toxicity, etc. Since brain endothelial cells and glioblastoma cells express lactoferrin receptors, a target-specific drug delivery vehicle was developed using lactoferrin itself as a matrix, into which carmustine was loaded. The objective was to use carmustine loaded lactoferrin nanoparticles (CLN) to achieve higher therapeutic efficacy and target specificity compared to free carmustine.

Methods: CLN were prepared using the Sol-oil method. The nanoparticles prepared were characterized for their size, shape, polydispersity, and stability using FESEM and DLS methods. Drug loading and drug releasing efficiencies were also estimated. Further, cellular uptake of nanoparticles and their antiproliferative efficacy against glioblastoma cells were evaluated.

Results: Characterization of CLN showed that they were spherical with ≤ 41 nm diameter and exhibited homogeneously dispersed stable distribution. Loading efficiency of carmustine in CLN was estimated to be 43±3.7 %. Drug release from the nanoparticles was pH dependent with the maximum observed at pH 5. At physiological and gastric pH, drug release was lower, whereas maximum release was observed at endocytotic vesicular and around tumor extracellular pH. Confocal microscopic studies showed an active cellular uptake of nanoparticles. Results of antiproliferative analysis substantiated a higher antiproliferative effect for CLN compared to free carmustine.

Conclusion: The results of the study demonstrated that CLN serves as a vital tool, in designing an effective treatment strategy for targeted drug delivery to glioblastoma.

Keywords: Lactoferrin nanoparticles, Carmustine, Glioblastoma, Drug delivery vehicle

DOI: http://dx.doi.org/10.22159/ijap.2018v10i6.28004

INTRODUCTION

Brain and other central nervous system tumors (BCNST), are known to be one of the leading causes of cancerous deaths. According to the central brain tumor registry of the United States (CBTRUS), in the US alone, every year on an average 15 000 deaths occur due to BCNST, and approximately 80 000 new cases are diagnosing yearly [1]. No known environmental risk factors other than ionizing radiation had identified for such higher incidence rates [2-4]. Amongst all the BCNST, glioblastoma is the most common and most aggressive malignant tumor with 5 y post-diagnosis survival rates of less than 6 % [1]. World health organization (WHO) grade IV classified, glioblastoma arises from malignantly transformed glial cells, and it diffusely invades other regions of the brain, making it highly lethal [5-7]. Its higher reoccurrence even after surgical resection adds to the complexity [8].

Current preferred treatment for glioblastoma is surgical resection of tumors, followed by radiotherapy with concurrent chemotherapy [9-13]. Despite these advanced treatments, there is no significant improvement reported in the overall survival rates of patients [8]. These failures are mainly due to (a) reoccurrence of tumors that arise from surgically inaccessible infiltrating malignant cells [8]; (b) emergence of resistance to radiotherapy and chemotherapy due to suboptimal dosage exposure for prolonged periods as a result of inefficient dosage delivery [14-17]; (c) higher systemic toxicity as a consequence of nonspecific localization of drugs [18-20]. These failures emphasize the need for the development of efficient drug delivery vehicles with significant drug localization in glioma cells.

In recent years, numerous efforts have been made to develop different drug delivery vehicles to overcome the above problems. Some of these are namely liposomes, nanoshells, dendrimers, solid lipid nanoparticles, polymeric micelles, carbon nanotubes, polyglycolic acid (PGA) nanoparticles, polylactic acid (PLA) nanoparticles, poly(D,L-lactic-co-glycolides) acid (PLGA) nanoparticles, polyanhydride nanoparticles, polyorthoesters nanoparticles, polycyanoacrylate nanoparticles, polycaprolactone nanoparticles, chitosan nanoparticles, albumin nanoparticles, etc. [21, 22]. But, many of these drug delivery vehicles lack target specificity, making their scope limited. Further, the poor ability of these vehicles in the transport of drugs across the blood-brain barrier significantly limits their application for delivery of drugs to the brain. Many strategies have developed to overcome the above limitations [22, 23]. Among them, exploiting one of the brain's natural transport systems, the receptor-mediated endocytosis, is gaining much interest in delivering therapeutic drugs to the brain. Ligands commonly used for this purpose are folate, transferrin, lactoferrin, etc. These ligands are either coated or conjugated to the nanoparticles, to facilitate nanoparticles entry into the brain via receptor-mediated endocytosis [23, 24].

Lactoferrin is an 80 kDa protein, which is mainly found in milk and other secretory body fluids. It has numerous clinically significant physiological functions viz., anti-inflammation, host defense against infections, maintenance of iron homeostasis, etc. [25-28]. Since brain endothelial cells, and glioblastoma cells [29-33] express lactoferrin receptors and also its low endogenous levels in serum [34, 35], make lactoferrin more advantageous in using it for targeting to the brain as it avoids competition with endogenous ligands and also increases target specificity. Drug-loaded nanoparticles were reported to possess a significant advantage over drug conjugated nanoparticles regarding efficacy and drug release in the targeted cells [36].

In the context of these facts, biodegradable protein nanoparticles were developed using lactoferrin itself as a matrix, into which chemotherapeutic drug, carmustine was loaded, and these nanoparticles were used for targeting brain tumors *in vitro*. The objective was to exploit lactoferrin nanoparticles for a dual purpose, as a drug carrier, as well as a targeting ligand. Cell culture models were used to evaluate the efficiency of carmustine loaded lactoferrin nanoparticles in drug localization and cytotoxicity.

We hypothesize that carmustine loaded lactoferrin nanoparticles will be an effective treatment strategy for targeting brain tumors if it increases target specificity, enhance therapeutic efficacy,

bioavailability, and stability, and also minimizes the systemic toxicity of the drug. This paper discusses the preparation of carmustine loaded lactoferrin nanoparticles, their optimal characteristic features which make them better drug delivery vehicles and further about their efficacy in treating brain tumors in general and more particularly glioblastoma *in vitro*.

MATERIALS AND METHODS

Materials

3-(4,5-dimethylthiazol-2-yl)-2,5-diphenyltetrazolium bromide (MTT), 4′,6-diamidino-2-phenylindole (DAPI), rhodamine 123 were procured from Sigma–Aldrich (St. Louis, USA), lactoferrin was obtained from Naturade LLC (Irvine, USA), and olive oil from Nicola pantaleo (Fasano, Italy). Carmustine was of pharmaceutical grade (Emcure pharmaceuticals, Pune, India). Minimum essential media, non-essential amino acids, sodium pyruvate, Dulbecco's modified eagle medium, fetal bovine serum were bought from Thermo fisher scientific (Waltham, USA). C_6 glioma, SK-N-SH cell lines were acquired from National centre for cell science (Pune, India). Rest of the materials were of either analytical or molecular biological grade.

Preparation of carmustine loaded lactoferrin, blank lactoferrin and rhodamine loaded lactoferrin nanoparticles

Nanoparticles were prepared as described by Krishna AD *et al.* (2009) [36]. Briefly, 1 ml of cold phosphate-buffered saline (PBS) pH-7.4 containing 50 mg of dissolved lactoferrin was gently mixed with 20 mg of carmustine dissolved in dimethyl sulfoxide (DMSO). The mixture was incubated at 4 °C for 30 min. After incubation, the mixture was slowly added to 30 ml of cold olive oil and was gently dispersed by vortexing, followed by sonication using ultrasonic homogenizer at 4 °C. Immediately the resulting mixture was snap frozen by keeping it in the liquid nitrogen for 10 min. After thawing the mixture at 4 °C, it was centrifuged at 8000 g for 15 min at 4 °C. The supernatant was discarded, and the pellet was washed thrice with diethyl ether. Following air drying, the pellet was dispersed in cold PBS (pH-7.4) by sonication and was stored at 4 °C until use. For fluorescent studies, rhodamine loaded lactoferrin nanoparticles were prepared similarly, but instead of carmustine, rhodamine was used. Similarly, blank lactoferrin nanoparticles were also prepared, but without the use of drug or dye.

Characterization of nanoparticles by field emission scanning electron microscope (FE-SEM)

Size and morphology of lactoferrin nanoparticles were characterized by FE-SEM (Field electron and ion, Hillsboro, USA). Freshly prepared lactoferrin nanoparticles were coated on a clean glass slide and were dried overnight in a dust-free chamber. Samples were then coated with gold and were viewed under the electron microscope. For image capturing and data analysis, the manufacturer's standard operative procedures were followed.

Characterization of nanoparticles by dynamic light scattering (DLS)

Zeta potential, hydrodynamic diameter, and polydispersity index (PDI) of lactoferrin nanoparticles in suspension form were analyzed by dynamic light scattering method using SZ-100 Nanopartica analyzer system equipped with a diode-pumped solid-state laser having a wavelength of 532 nm (Horiba scientific, Irvine, USA). Particle analysis and data acquisition were carried out according to the manufacturer's instructions.

Evaluation of loading efficiency

Carmustine loaded lactoferrin nanoparticles were suspended in 1 ml of PBS of pH-5 and were kept under gentle rocking at 4 °C for 30 min for the release of the drug from the nanoparticles (n = 3). 30 % silver nitrate was added to precipitate the protein out of the solution. The resulting solution was centrifuged at 15 000 g for 15 min at 4 °C. The obtained supernatant was filtered and used for the drug estimation by high-performance liquid chromatography (HPLC) (Waters, Milford, USA) [37]. The supernatant was analyzed in triplicate. Different concentrations of carmustine solutions were also prepared and estimated by HPLC to develop a standard curve. Amount of carmustine loaded in the lactoferrin nanoparticles was determined using the developed standard curve.

Drug loading efficiency was calculated using the following formula.

$$\text{Loading efficiency \%} = (D_{Loaded}/D_{Total}) \times 100$$

$$D_{Loaded} = D_{Total} - D_{Lost}$$

where D_{Loaded} = amount of loaded drug; D_{Total} = amount of total drug used; D_{Lost} = amount of drug lost during preparation.

In vitro pH-dependent drug release assay

pH-dependent drug release assay was performed by quantifying drug released under different pH conditions [38]. Pelleted nanoparticles equivalent to 200 µg of carmustine were suspended in PBS solutions of varying pH ranges (1-9) and were incubated for 4 h at 4 °C on a rocker with moderate speed. After incubation, 30 % silver nitrate was added to the PBS solutions to precipitate protein. The mobile phase was also added to extract the drug, followed by centrifugation at 15000 g for 15 min at 4 °C. The obtained supernatant was filtered using a 0.2-micron filter, and the amount of drug present in the supernatant was estimated using HPLC at 230 nm wavelength for carmustine. For quantification of unknown amounts of the drug in the samples, a standard curve was developed using known concentrations of the drug in the same incubation media and quantified by HPLC. Each sample was quantified in triplicate (n = 3).

Cellular uptake assay by confocal microscopy

SK-N-SH cells (seeding density of 2×10^5 cells) were grown on glass coverslips in 12 well plates. Equivalent amounts of rhodamine loaded lactoferrin nanoparticles were added to the wells and were incubated for different time points (0.5 h, 1 h, 2 h, 4 h, and 8 h). Untreated cells were kept as control. After specified time points, cells were washed thrice with PBS buffer (pH-7.4) and were fixed with 4 % paraformaldehyde for 10 min. After subsequent washings with PBS buffer, cells were counterstained with DAPI, and the coverslips were mounted on a glass slide. Cells were viewed under the confocal microscope (Leica, Buffalo grove, USA) for analyzing the amount of uptake of nanoparticles, by utilizing the intrinsic fluorescence of rhodamine 123 (excitation and emission maxima are 511 nm and 534 nm respectively) [39].

Evaluation of the antiproliferative activity of carmustine loaded lactoferrin nanoparticles

The antiproliferative assay was performed using the MTT method [40]. Briefly, 50 000 C6 glioma cells were seeded in every well of the 96 well plate and were incubated in the carbon dioxide incubator at 37 °C for 12 h. After incubation, media was replaced with fresh media containing increasing concentrations of either soluble carmustine or its equivalent carmustine loaded nanoparticles. Similar treatment was given with blank lactoferrin nanoparticles. Control cells were also kept, without the addition of neither soluble drug nor the nanoparticles. Cells were incubated in the 37 °C carbon dioxide incubator for 24 h. After incubation, media was discarded, and cells were washed twice. Fresh media containing 10 %, 5 mg/ml MTT, was added to the cells followed by incubation for 8 h in a carbon dioxide incubator at 37 °C. During incubation, cells that survived after the treatment convert yellow tetrazolium salt into insoluble formazan crystals. MTT containing media was discarded, and insoluble formazan crystals were dissolved by the addition of DMSO. The intensity of the developed color was measured using multiplate reader-Infinite 200 (Tecan, Mannedorf, Switzerland) at 595 nm. Percentage of inhibition (PI) was calculated according to the following formula.

$$PI = \{(OD_{Control} - OD_{Treated})/OD_{Control}\} \times 100$$

where, PI = percentage of inhibition; $OD_{Control}$ = absorbance at 595 nm for control cells; $OD_{Treated}$ = absorbance at 595 nm for treated cells.

After plotting the graph, half maximal inhibitory concentration (IC_{50} value) was calculated from it.

Statistics

All the experiments were performed a minimum of three times individually. Data were presented as mean±standard deviation. Amounts of drug released at various pH conditions were statistically analyzed by one-way ANOVA using the Student-Newman-Keuls

method. Antiproliferative activities of free carmustine and carmustine loaded lactoferrin nanoparticles were statistically compared by Student t-test. P<0.05 was regarded as statistically significant.

RESULTS

Characterization of nanoparticles by FESEM

Blank lactoferrin nanoparticles and carmustine loaded lactoferrin nanoparticles were prepared as described in materials and methods. The prepared nanoparticles were characterized by FESEM to obtain information relating to their size and morphology. The FESEM analysis revealed that their sizes were in the range of 13-22 nm, with an average size of 17.5±3.06 nm (mean±SD) for blank lactoferrin nanoparticles (fig. 1a) and in the range of 32-41 nm, with an average size of 36.5±3.90 nm (mean±SD) for carmustine loaded lactoferrin nanoparticles (fig. 1b). It is apparent that lactoferrin nanoparticles become more than double in their average size after loading of the drug. Further, FESEM analysis revealed that the nanoparticles were homogenous in their sizes and were spherical in their shapes.

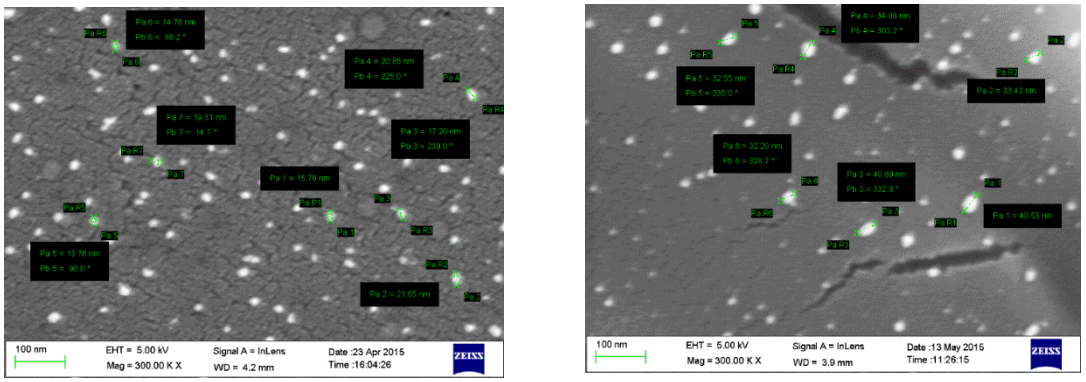

(A) **(B)**

Fig. 1: FESEM analysis of (A) blank lactoferrin nanoparticles, (B) carmustine loaded lactoferrin nanoparticles. Above image was representative of a quadruplicate experiment (n = 4)

Characterization of nanoparticles by DLS

Zeta potential values of blank lactoferrin nanoparticles and carmustine loaded lactoferrin nanoparticles were -14.9±3.87 mV (mean±SD) (fig. 2a) and -24.6±5.94 mV (mean±SD) (fig. 2b) respectively. These zeta potential values indicate that carmustine loaded lactoferrin nanoparticles were under colloidal stability in nature, and blank lactoferrin nanoparticles were under moderately colloidal stability in nature. Hydrodynamic sizes of nanoparticles were also investigated using DLS analysis (fig. 2c and fig. 2d). Since DLS measures the hydrodynamic diameter of the particles, whereas FESEM measures size in the dry state, nanoparticles sizes were little larger in DLS compared to FESEM analysis. PDI for blank lactoferrin nanoparticles was 0.264±0.03 and for carmustine loaded lactoferrin nanoparticles was 0.338±0.05. These PDI values confirm that these nanoparticles had a homogeneously dispersed size distribution.

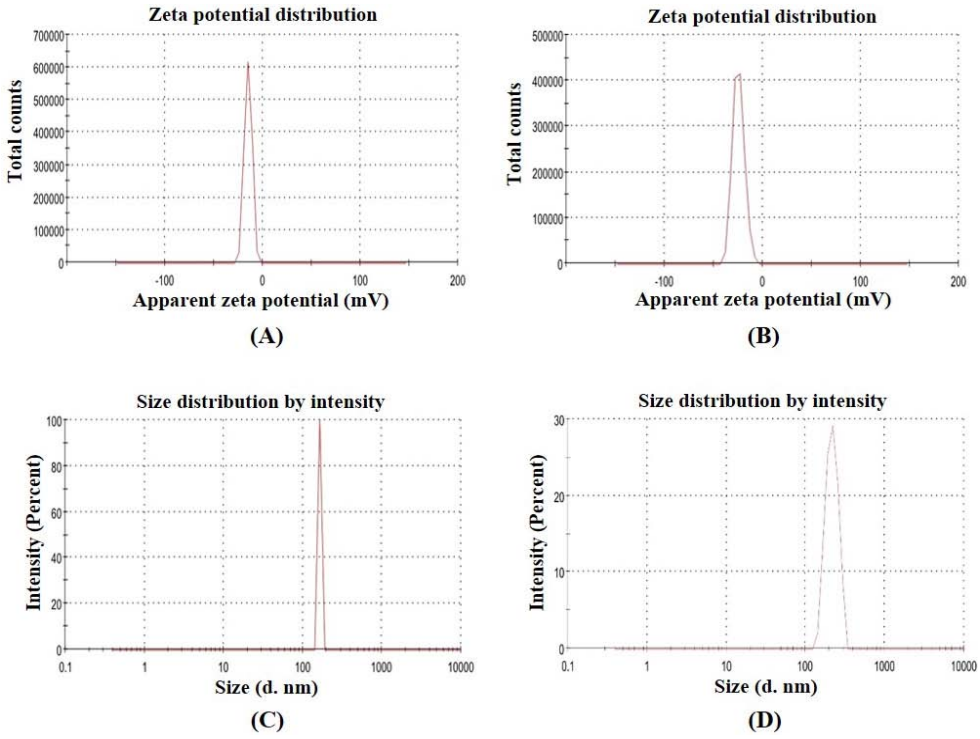

Fig. 2: DLS analysis: Zeta potential measurements of (A) blank lactoferrin nanoparticles, (B) carmustine loaded lactoferrin nanoparticles. Hydrodynamic diameter measurements of (C) blank lactoferrin nanoparticles, (D) carmustine loaded lactoferrin nanoparticles. The experiment was conducted in triplicates (n = 3)

Estimation of drug loading efficiency of carmustine loaded lactoferrin nanoparticles

Significantly higher drug loading efficiency was achieved in the nanoparticles by using the Sol-oil method. Carmustine solutions of different concentrations were prepared and estimated by HPLC, and the standard graph was developed for calculating the amount of encapsulated carmustine present in the lactoferrin nanoparticles (fig. 3b). Carmustine loaded lactoferrin nanoformulations were treated as described in the materials and methods, the released drug was estimated by HPLC (fig. 3a) and correlated with the standard graph. Then the loading efficiencies were calculated using the formula mentioned in the materials and methods. Loading efficiency of carmustine in the carmustine loaded lactoferrin nanoparticles was found to be 43±3.7 % (n = 3).

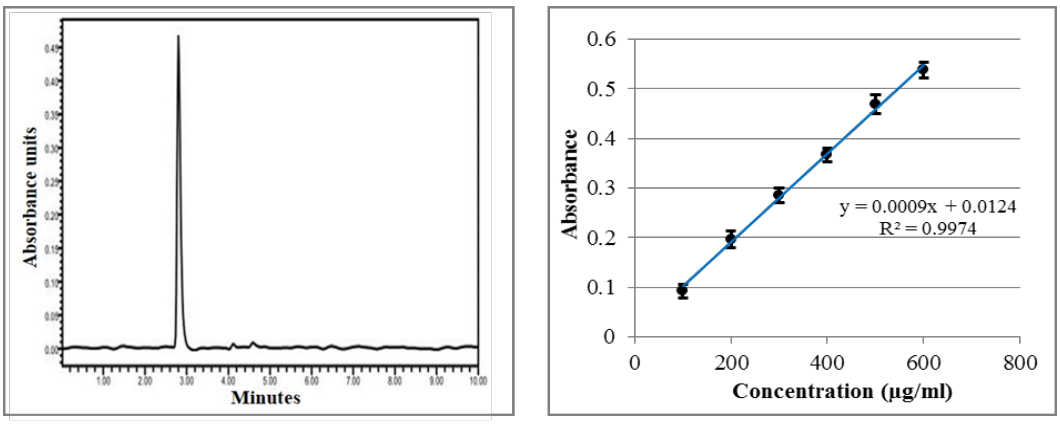

(A) (B)

Fig. 3: (A) HPLC analysis of carmustine at 230 nm wavelength. (B) Quantification of carmustine by HPLC; data were represented as mean±SD (n = 3)

***In vitro* pH-dependent drug release assay**

pH-dependent release assay of carmustine loaded lactoferrin nanoparticles were carried out at various pH ranges (1–9) (fig. 4). The maximum amount of drug was released at pH 5, which was followed by pH 6. At all other pH conditions, the release was comparatively low. At physiological pH (pH 7.2 to 7.4) and gastric pH (pH 1 to 2.5), drug release was less than 20 % and whereas maximum release was observed at endocytotic vesicular pH (pH 5) and around tumor extracellular pH (pH 5.85-7.35) [41], from the nanoparticles.

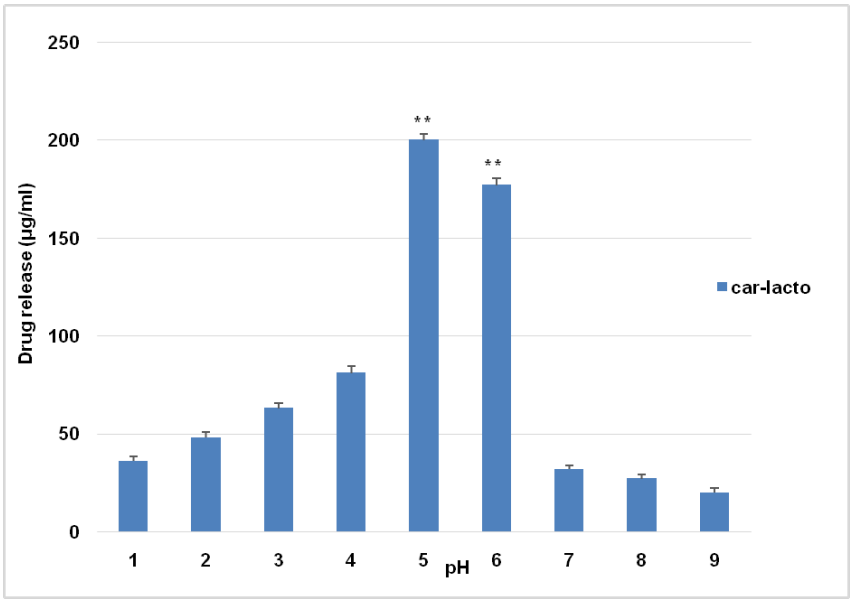

Fig. 4: pH-dependent release assay of carmustine loaded lactoferrin nanoparticles. Car-lacto represents carmustine loaded lactoferrin nanoparticle. Averages and standard deviations from three experiments (n = 3) were shown as mean±SD. **P<0.01 by one-way ANOVA using Student-Newman-Keuls method

Cellular uptake assay by confocal microscopy

Rhodamine 123 loaded lactoferrin nanoparticles were incubated with the cells for different time points to confirm the cellular uptake of nanoparticles. Up to 1 h of incubation, rhodamine was not visible, but after 2 h, it was noticed that its level had increased with the increment of time. By the end of 8 h, cells were localized entirely with rhodamine 123. Cells, which were not exposed to rhodamine 123 loaded nanoparticles, were taken as the control (fig. 5). Time

course experiment showed that there was a gradual increase of rhodamine in the cells with the time, which confirmed the cellular uptake of nanoparticles and their rise was gradual and proportional to the time. This result also confirmed the longer retention of lactoferrin nanoparticles within the cells, which provides a longer time for chemotherapeutic drugs to confer the antiproliferative effect.

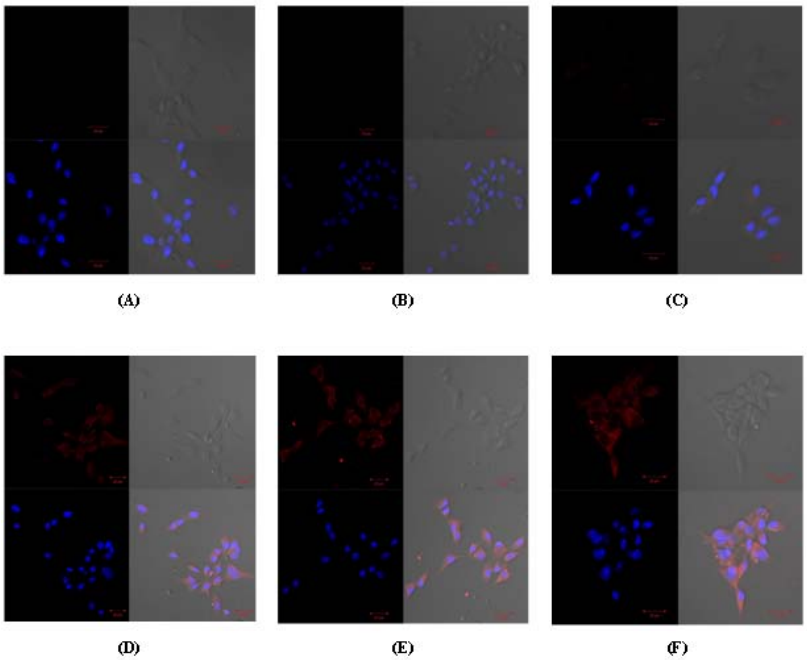

Fig. 5: Cellular uptake of rhodamine 123 loaded lactoferrin nanoparticles. Time course experiment showed the uptake of nanoparticles into the cells, and there was a gradual increase in the uptake of nanoparticles with the increment of time. A, B, C, D, E, F represent control, 0.5 h, 1h, 2h, 4h, and 8h time points respectively. In each big square, the upper left square represents the rhodamine 123 (red), the upper right square represents transmission image, the lower left square represents DAPI (blue), and the lower right square represents merger image. Total number of independent experimentation, n = 3

Evaluation of the antiproliferative activity of carmustine loaded lactoferrin nanoparticles

Antiproliferative activity of carmustine loaded lactoferrin nanoparticles were compared with the antiproliferative activity of the free drug (carmustine) after 24 h of treatment with free drug and drug-loaded nanoparticles. The results clearly showed that carmustine loaded lactoferrin nanoparticles had a higher antiproliferative effect compared to free carmustine at all the experimental concentrations (fig. 6a). And there was a reduction of 3.29 times in the IC_{50} value with the treatment of carmustine loaded lactoferrin nanoparticles compared to free carmustine treatment. IC_{50} values of free carmustine and carmustine loaded lactoferrin nanoparticles were 43.22 µg/ml and 12.76 µg/ml respectively. Blank lactoferrin nanoparticles (delivery vehicle) didn't show any significant antiproliferative activity at all the experimental concentrations (fig. 6b).

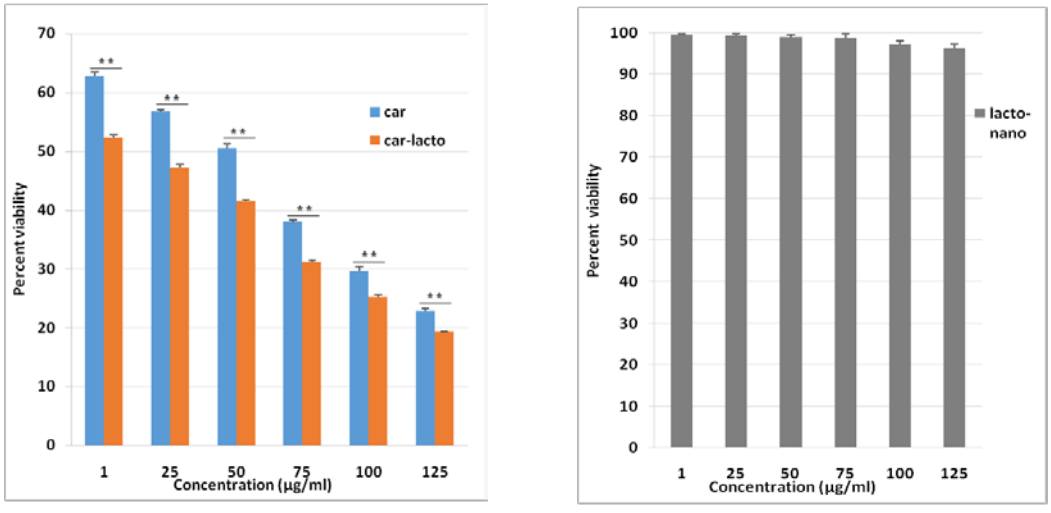

Fig. 6: Dose-dependent antiproliferative activities of (A) free carmustine and carmustine loaded lactoferrin nanoparticles and (B) free lactoferrin nanoparticles after 24 h of treatment. Car, car-lacto, and lacto-nano represent the treatment of carmustine drug, carmustine

loaded lactoferrin nanoparticles and blank lactoferrin nanoparticles respectively. Data were represented as mean±SD (n = 3), **P<0.01 by student t-test

DISCUSSION

Current advanced treatments for glioblastoma remain not so effective since there is no significant improvement in the survival of the patients. The purpose of this study was to develop an effective target-specific drug delivery vehicle with reduced systemic toxicity and increased therapeutic efficacy against glioblastoma. As it is known, lactoferrin receptors are expressed on brain endothelial cells, and glioblastoma cells, a target-specific drug delivery vehicle was developed, using lactoferrin itself as a matrix, into which chemotherapeutic drug, carmustine was loaded. In the present study, carmustine loaded lactoferrin nanoparticles were prepared and characterized their features such as size, shape, polydispersity, stability, drug loading efficiency, drug releasing efficiency, cellular uptake ability, etc., and further evaluated their efficacy in treating glioblastoma.

For decades, carmustine was a drug of choice for treating glioblastoma [42-44]. Due to its dose-limiting side effects such as bone marrow suppression [45] and non-dose dependent pulmonary fibrosis [46], its usage was limited. To reduce systemic toxicity, intracranial polymer implants (gliadel wafers) impregnated with carmustine, have been using clinically since 1996 [19]. But these gliadel wafers were found to be not successful as they do not show effective therapeutic efficacy due to many limitations such as lower penetration, inability in preventing short distant tumor recurrence, lack of synergetic action in combination with radiotherapy and other chemotherapeutic drugs, practical difficulties in prescribing regular dosage schedules as it requires regular intracranial surgeries [47, 19]. Further, complications are reported in the use of gliadel wafers due to severe adverse effects such as healing abnormalities [48], craniotomy infections [49], seizures [11], oedema [11, 50], neurological decline [50], intracranial hypertension [10], cerebrospinal fluid leaks [10], tumor bed cyst formation [51], pericavity necrosis [52] etc. These limitations and adverse effects emphasize the need for a better drug delivery vehicle for efficient treatment of glioblastoma.

In the present study, carmustine loaded lactoferrin nanoparticles were prepared using the Sol-oil method. This method is simple, less time consuming and doesn't involve any chemical modifications either to the drug or protein unlike other methods such as protein coacervation method [53]. Further, lactoferrin conformation remains in the native state. As the nanoparticles are prepared using lactoferrin, a natural protein present abundantly in milk and other secretory body fluids, these nanoparticles are safer to use even at high dosages. Besides, significantly higher drug loading efficiency was also achieved in the nanoparticles by using this method. Drug loading was indeed higher compared to commercially available carmustine implants, which have only 3.85 % drug loading capacity [11]. The reported maximum drug loading capacity that can be achieved in the biodegradable polymers was 28 % [54], which was less than that observed in carmustine loaded lactoferrin nanoparticles (43±3.7 %). Drug loading efficiency of a drug delivery vehicle can influence its therapeutic index. Higher the achieved drug loading efficiency, higher will be the therapeutic index. With the increased therapeutic index there will be an enhanced antitumor effect and reduced toxicity [55].

Using Sol-oil method, nanoparticles of sizes ≤ 41 nm were successfully developed, which was confirmed by FESEM analysis. FESEM studies also showed that blank lactoferrin nanoparticles of 13-22 nm size became enlarged to 32-41 nm size after successful loading of carmustine drug. It is an advantage to have smaller sized nanoparticles because several studies had consistently shown that smaller sized nanoparticles were capable of escaping from the reticuloendothelial system, thereby evaded rapid clearance from systemic circulation and had longer circulation time and stability in the blood [56-59]. Several other studies also had shown, an inverse correlation between nanoparticle size's and blood-brain barrier penetration [60-62]. It indicates that particles, which are smaller in size can cross the blood-brain barrier more efficiently than particles which are larger. Thus, the smaller size of these nanoparticles can increase their circulatory half-life and also make them more efficient in crossing the blood-brain barrier.

The measured zeta potential values indicate that these nanoparticles were stable. Carmustine loaded lactoferrin nanoparticles were under colloidal stability range, whereas blank lactoferrin nanoparticles were under moderately colloidal stability range. Measured nanoparticle sizes were found to be little larger in DLS compared to FESEM analysis. Since, DLS measures the hydrodynamic diameter of the particle, which includes not only the particle but also the ionic and solvent layers associated with the particle in the solution, the particle sizes will be larger in DLS compared to FESEM, which measures size in the dry state [63, 64]. Polydispersity index values of 0.264±0.03 and 0.338±0.05 for blank lactoferrin nanoparticles and carmustine loaded lactoferrin nanoparticles respectively indicate that these nanoparticles possess a homogenous population with narrow size distribution.

The release of the drug from the nanoparticles was found to be pH dependent. It was observed that at physiological and gastric pH, drug release from the nanoparticles was very minimum, whereas maximum drug release was observed at the endocytotic vesicular pH (pH 5) and around tumor extracellular pH (pH 5.85-7.35) [41], which indicates that these nanoparticles can have low loss of the drug during systemic circulation, thereby exhibit reduced systemic toxicity. And they also show more specificity in the drug release, mainly in the endocytotic vesicles, which are involved in receptor-mediated endocytosis and around tumor environment, which have reduced pH as a consequence of higher anaerobic respiration of cancerous cells [65, 66]. pH-dependent drug release is an added advantage, which makes these nanoparticles optimal drug delivery vehicles with reduced systemic toxicity and increased tumor specificity.

As carmustine drug was nonfluorescent, cellular uptake of nanoparticles was tested by loading fluorescent dye, rhodamine 123 into the lactoferrin nanoparticles. Time course study using confocal microscopy had shown that there was a gradual increase of rhodamine in the cells with the increment of time, which confirmed the active cellular uptake of lactoferrin nanoparticles. Earlier it was reported that the mechanism of uptake of lactoferrin nanoparticles into the cells was through receptor-mediated endocytosis [36, 39]. As the brain endothelial cells and glioblastoma cells express lactoferrin receptors [29-33], a similar mechanism could be operative, during the transport of carmustine loaded lactoferrin nanoparticles across the blood-brain barrier and also at the entry into the tumor cells.

Comparative study of the antiproliferative effect of free carmustine and carmustine loaded lactoferrin nanoparticles, had validated that carmustine loaded lactoferrin nanoparticles had a higher therapeutic efficacy than free carmustine. Previously, carmustine encapsulated liposomes, and carmustine-magnetic nanoparticles showed 50 % inhibition at around 467 μM and 100 μM concentrations of carmustine respectively [67, 68], whereas carmustine loaded lactoferrin nanoparticles showed 50 % inhibition at 59.6 μM of carmustine, which was significantly lower and further substantiates the higher therapeutic efficacy of carmustine loaded lactoferrin nanoparticles. These results were also consistent with the earlier reports [39, 38], where lactoferrin nanoparticles had used as drug delivery vehicles. Higher uptake of nanoparticles, sustained drug release from the nanoparticles and the longer retention of the drug inside the cells might have contributed to the increased therapeutic efficacy of carmustine loaded lactoferrin nanoparticles against C6 glioma cells compared to the free carmustine.

Current state of the art, drug delivery vehicles for the treatment of glioblastoma includes solid lipid nanoparticles, nanostructured lipid carriers, liposomes, polymeric nanoparticles, micelles, magnetic nanoparticles, gold nanoshells, carbon nanotubes, etc. These drug delivery vehicles are failing to be an effective therapeutics due to one or more of the crucial issues viz., lower encapsulation efficiency, higher toxicity, lower stability, rapid clearance from the blood, lower biodegradability, lack of specificity, lower therapeutic indices, higher manufacturing costs, etc. [69-71, 21]. But, as may be seen from the results of the present study, carmustine loaded lactoferrin

nanoparticles are showing promising results, which may overcome these challenges.

Thus, carmustine loaded lactoferrin nanoparticles serve as potential drug delivery vehicles in treating glioblastoma effectively *in vitro*. Further studies are required to establish *in vivo* efficacy.

CONCLUSION

Carmustine loaded lactoferrin nanoparticles, with ≤ 41 nm size were successfully developed, using lactoferrin as a single matrix. These nanoparticles were spherical with homogeneous distribution, enhanced stability, and higher drug loading efficiency. The release of the drug from nanoparticles was pH dependent, which adds additional advantage to this target specific drug delivery vehicle. Further, active cellular uptake of nanoparticles with a significant antiproliferative effect in cell culture models substantiated carmustine loaded nanoparticles as an effective drug delivery vehicle in treating glioblastoma.

Further *in vivo* efficacy and toxicological studies using carmustine loaded lactoferrin nanoparticles would provide an opportunity for the development of an effective treatment strategy against glioblastoma without any systemic toxicity.

ACKNOWLEDGEMENT

Authors are thankful to the Indian Council of Medical Research and Department of Science and Technology, India for providing the grant for this work. Authors are grateful to the University Grants Commission, India and the Department of Biotechnology-Centre for Research and Education in Biology and Biotechnology program of the University of Hyderabad, India for providing the infrastructure for this work. Authors are also thankful to the Council of Scientific and Industrial Research, India for providing doctoral fellowship to Harikiran.

AUTHORS CONTRIBUTIONS

Harikiran performed all experiments, compiled data, and drafted manuscript. Anand Kumar planned experiments, analyzed results and edited manuscript. All the authors have approved the final article.

CONFLICT OF INTERESTS

Declared none

REFERENCES

1. Ostrom QT, Gittleman H, Liao P, Vecchione-Koval T, Wolinsky Y, Kruchko C, *et al.* CBTRUS statistical report: primary brain and other central nervous system tumors diagnosed in the united states in 2010-2014. Neurol Oncol 2017;19 Suppl 5:1-88.
2. Johnson KJC, Cullen J, Barnholtz Sloan JS, Ostrom QT, Langer CE, Turner MC, *et al.* Childhood brain tumor epidemiology: a brain tumor epidemiology consortium review. Cancer Epidemiol Biomarkers Prev 2014;23:2716-36.
3. Ostrom QT, Bauchet L, Davis FG, Deltour I, Fisher JL, Langer CE, *et al.* The epidemiology of glioma in adults: a state of the science review. Neurol Oncol 2014;16:896-913.
4. Wiemels J, Wrensch M, Claus EB. Epidemiology and etiology of meningioma. J Neurooncol 2010;99:307-14.
5. Louis DN, Ohgaki H, Wiestler OD, Cavenee WK, Burger PC, Jouvet A, *et al.* The 2007 WHO classification of tumours of the central nervous system. Acta Neuropathol 2007;114:97–109.
6. Quirk BJ, Brandal G, Donlon S, Vera JC, Mang TS, Foy AB, *et al*. Photodynamic therapy (PDT) for malignant brain tumors–where do we stand? Photodiagnosis Photodyn Ther 2015;12:530-44.
7. Omuro A, DeAngelis LM. Glioblastoma and other malignant gliomas: a clinical review. JAMA 2013;310:1842-50.
8. Demuth T, Berens ME. Molecular mechanisms of glioma cell migration and invasion. J Neurooncol 2004;70:217-28.
9. Stupp R, Mason WP, Van den Bent MJ, Weller M, Fisher B, Taphoorn MJ, *et al.* Radiotherapy plus concomitant and adjuvant temozolomide for glioblastoma. N Engl J Med 2005;352:987-96.
10. Westphal M, Hilt DC, Bortey E, Delavault P, Olivares R, Warnke PC, *et al.* A phase 3 trial of local chemotherapy with biodegradable carmustine (BCNU) wafers (gliadel wafers) in patients with primary malignant glioma. Neurol Oncol 2003;5:79-88.
11. Brem H, Piantadosi S, Burger PC, Walker M, Selker R, Vick NA, *et al.* Placebo-controlled trial of safety and efficacy of intraoperative controlled delivery by biodegradable polymers of chemotherapy for recurrent gliomas. Lancet 1995;345:1008-12.
12. Patel MA, Kim JE, Ruzevick J, Li G, Lim M. The future of glioblastoma therapy: synergism of standard of care and immunotherapy. Cancers 2014;6:1953-85.
13. Woodworth GF, Dunn GP, Nance EA, Hanes J, Brem H. Emerging insights into barriers to effective brain tumor therapeutics. Front Oncol 2014;4:1-14.
14. Bao S, Wu Q, McLendon RE, Hao Y, Shi Q, Hjelmeland AB, *et al.* Glioma stem cells promote radioresistance by preferential activation of the DNA damage response. Nature 2006;444:756-60.
15. Beier D, Schulz JB, Beier CP. Chemoresistance of glioblastoma cancer stem cells-much more complex than expected. Mol Cancer 2011;10:1-11.
16. Sarkaria JN, Kitange GJ, James CD, Plummer R, Calvert H, Weller M, *et al.* Mechanisms of chemoresistance in malignant glioma. Clin Cancer Res 2008;14:2900-8.
17. Zhang J, Stevens MF, Laughton CA, Madhusudan S, Bradshaw TD. Acquired resistance to temozolomide in glioma cell lines: molecular mechanisms and potential translational applications. Oncology 2010;78:103-14.
18. Blakeley J, Grossman SA. Chemotherapy with cytotoxic and cytostatic agents in brain cancer. In: Aminoff MJ, Boller F, Swaab DF, editors. Handbook of Clinical Neurology. Elsevier; 2012. p. 229-54.
19. Lin SH, Kleinberg LR. Carmustine wafers: localized delivery of chemotherapeutic agents in CNS malignancies. Expert Rev Anticancer Ther 2008;8:343-59.
20. Chamberlain MC. Temozolomide: therapeutic limitations in the treatment of adult high-grade gliomas. Expert Rev Neurother 2010;10:1537-44.
21. Krupa P, Rehak S, Diaz-Garcia D, Filip S. Nanotechnology-new trends in the treatment of brain tumors. Acta Med 2014;57:142-50.
22. Invernici G, Cristini S, Alessandri G, Navone SE, Canzi L, Tavian D, *et al.* Nanotechnology advances in brain tumors: the state of the art. Recent Pat Anticancer Drug Discovery 2011;6:58-69.
23. Rempe R, Cramer S, Qiao R, Galla HJ. Strategies to overcome the barrier: use of nanoparticles as carriers and modulators of barrier properties. Cell Tissue Res 2014;355:717-26.
24. Chang J, Paillard A, Passirani C, Morille M, Benoit JP, Betbeder D, *et al.* Transferrin adsorption onto PLGA nanoparticles governs their interaction with biological systems from blood circulation to brain cancer cells. Pharm Res 2012;29:1495-505.
25. Nuijens JH, Van Berkel PHC, Schanbacher FL. Structure and biological actions of lactoferrin. J Mammary Gland Biol Neoplasia 1996;1:285-95.
26. Ward PP, Paz E, Conneely OM. Multifunctional roles of lactoferrin: a critical overview. Cell Mol Life Sci 2005;62:2540-8.
27. Moreno-Exposito L, Illescas-Montes R, Melguizo-Rodriguez L, Ruiz C, Ramos-Torrecillas J, de Luna-Bertos E. Multifunctional capacity and therapeutic potential of lactoferrin. Life Sci 2018;195:61-4.
28. Jayasinghe S, Siriwardhana A, Karunaratne V. Natural iron sequestering agents: their roles in nature and therapeutic potential. Int J Pharm Pharm Sci 2015;7:8-12.
29. Huang RQ, Ke WL, Qu YH, Zhu JH, Pei YY, Jiang C. Characterization of lactoferrin receptor in brain endothelial capillary cells and mouse brain. J Biomed Sci 2007;14:121-8.
30. Ji B, Maeda J, Higuchi M, Inoue K, Akita H, Harashima H, *et al.* Pharmacokinetics and brain uptake of lactoferrin in rats. Life Sci 2006;78:851-5.
31. Fillebeen C, Descamps L, Dehouck M, Fenart L, Benaıssa M, Spik G, *et al.* Receptor-mediated transcytosis of lactoferrin through the blood-brain barrier. J Biol Chem 1999;274:7011–7.

32. Qiao R, Jia Q, Huwel S, Xia R, Liu T, Gao F, *et al.* Receptor-mediated delivery of magnetic nanoparticles across the blood-brain barrier. ACS Nanol 2012;6:3304-10.
33. Fang JH, Lai YH, Chiu TL, Chen YY, Hu SH, Chen SY. Magnetic core-shell nanocapsules with dual-targeting capabilities and co-delivery of multiple drugs to treat brain gliomas. Adv Healthc Mater 2014;3:1250-60.
34. Talukder MJ, Takeuchi T, Harada E. Characteristics of lactoferrin receptor in bovine intestine: higher binding activity to the epithelium overlying Peyer's patches. J Vet Med A Physiol Pathol Clin Med 2003;50:123-31.
35. Sanchez L, Calvo M, Brock JH. Biological role of lactoferrin. Arch Dis Child 1992;67:657-61.
36. Krishna AD, Mandraju RK, Kishore G, Kondapi AK. An efficient targeted drug delivery through apotransferrin loaded nanoparticles. PLoS One 2009;4:e7240.
37. Lakshmi YS, Kumar P, Kishore G, Bhaskar C, Kondapi AK. Triple combination MPT vaginal microbicide using curcumin and efavirenz loaded lactoferrin nanoparticles. Sci Rep 2016;6:25479.
38. Kumari S, Kondapi AK. Lactoferrin nanoparticle mediated targeted delivery of 5-fluorouracil for enhanced therapeutic efficacy. Int J Biol Macromol 2017;95:232-7.
39. Ahmed F, Ali MJ, Kondapi AK. Carboplatin loaded protein nanoparticles exhibit improve anti-proliferative activity in retinoblastoma cells. Int J Biol Macromol 2014;70:572-82.
40. Mosmann T. Rapid colorimetric assay for cellular growth and survival: application to proliferation and cytotoxicity assays. J Immunol Methods 1983;65:55-63.
41. Wike Hooley JL, Haveman J, Reinhold HS. The relevance of tumour pH to the treatment of malignant disease. Radiother Oncol 1984;2:343-66.
42. Weiss RB, Issell BF. The nitrosoureas: carmustine (BCNU) and lomustine (CCNU). Cancer Treat Rev 1982;9:313-30.
43. Chang CH, Horton J, Schoenfeld D, Salazer O, Perez-Tamayo R, Kramer S, *et al.* Comparison of postoperative radiotherapy and combined postoperative radiotherapy and chemotherapy in the multidisciplinary management of malignant gliomas. Cancer 1983;52:997-1007.
44. Selker RG, Shapiro WR, Burger P, Blackwood MS, Arena VC, Gilder JC, *et al.* The brain tumor cooperative group NIH trial 87-01:a randomized comparison of surgery, external radiotherapy, and carmustine versus surgery, interstitial radiotherapy boost, external radiation therapy, and carmustine. Neurosurgery 2002;51:343-57.
45. De Vita VT, Carbone PP, Owens AH, Gold GL, Krant MJ, Edmonson J. Clinical trials with 1, 3-bis(2-chloroethyl)-1-nitrosourea, NSC-409962. Cancer Res 1965;25:1876-81.
46. O'Driscoll BR, Kalra S, Gattamaneni HR, Woodcock AA. Late carmustine lung fibrosis. Age at treatment may influence severity and survival. Chest 1995;107:1355-7.
47. Bota DA, Desjardins A, Quinn JA, Affronti ML, Friedman HS. Interstitial chemotherapy with biodegradable BCNU (gliadel) wafers in the treatment of malignant gliomas. Ther Clin Risk Manag 2007;3:707-15.
48. Subach BR, Witham TF, Kondziolka D, Lunsford LD, Bozik M, Schiff D. Morbidity and survival after 1,3-bis(2-chloroethyl)-1-nitrosourea wafer implantation for recurrent glioblastoma: a retrospective case-matched cohort series. Neurosurgery 1999;45:17-22.
49. McGovern PC, Lautenbach E, Brennan PJ, Lustig RA, Fishman NO. Risk factors for postcraniotomy surgical site infection after 1,3-bis (2-chloroethyl)-1-nitrosourea (gliadel) wafer placement. Clin Infect Dis 2003;36:759-65.
50. Weber EL, Goebel EA. Cerebral edema associated with gliadel wafers: two case studies. Neurol Oncol 2005;7:84-9.
51. Engelhard HH. Tumor bed cyst formation after BCNU wafer implantation: report of two cases. Surg Neurol 2000;53:220-4.
52. Kleinberg LR, Weingart J, Burger P, Carson K, Grossman SA, Li K, *et al.* Clinical course and pathologic findings after gliadel and radiotherapy for newly diagnosed malignant glioma: implications for patient management. Cancer Invest 2004;22:1-9.
53. Shome D, Poddar N, Sharma V, Sheorey U, Maru GB, Ingle A, *et al.* Does a nanomolecule of carboplatin injected periocularly help in attaining higher intravitreal concentrations? Invest Ophthalmol Vis Sci 2009;50:5896-900.
54. Olivi A, Grossman SA, Tatter S, Barker F, Judy K, Olsen J, *et al.* Dose escalation of carmustine in surgically implanted polymers in patients with recurrent malignant glioma: a new approaches to brain tumor therapy CNS consortium trial. J Clin Oncol 2003;21:1845-9.
55. Sharma A, Sharma US. Liposomes in drug delivery: progress and limitations. Int J Pharm 1997;154:123-40.
56. Alexis F, Pridgen E, Molnar LK, Farokhzad OC. Factors affecting the clearance and biodistribution of polymeric nanoparticles. Mol Pharm 2008;5:505-15.
57. Masserini M. Nanoparticles for brain drug delivery. ISRN Biochem 2013;2013:1-18.
58. Ferroni L, Gardin C, Puppa DA, Sivolella S, Brunello G, Scienza R, *et al.* Novel nanotechnologies for brain cancer therapeutics and imaging. J Biomed Nanotechnol 2015;11:1899-912.
59. Hemant K, Raizaday A, Sivadasu P, Uniyal S, Kumar SH. Cancer nanotechnology: nanoparticulate drug delivery for the treatment of cancer. Int J Pharm Pharm Sci 2015;7:40-6.
60. Sonavane G, Tomoda K, Makino K. Biodistribution of colloidal gold nanoparticles after intravenous administration: effect of particle size. Colloids Surf B 2008;66:274-80.
61. Etame AB, Smith CA, Chan WC, Rutka JT. Design and potential application of PEGylated gold nanoparticles with size-dependent permeation through brain microvasculature. Nanomedicine 2011;7:992-1000.
62. Hanada S, Fujioka K, Inoue Y, Kanaya F, Manome Y, Yamamoto K. Cell-based *in vitro* blood-brain barrier model can rapidly evaluate nanoparticles brain permeability in association with particle size and surface modification. Int J Mol Sci 2014;15:1812-25.
63. Williams PM, Oatley-Radcliffe DL, Hilal N. Feed solution characterization. In: Hilal N, Ismail AF, Matsuura T, Oatley-Radcliffe D. editors. Membrane characterization. Elsevier; 2017. p. 379-404.
64. Uskokovic V. Dynamic light scattering based microelectrophoresis: main prospects and limitations. J Dispers Sci Technol 2012;33:1762-86.
65. Gatenby RA, Gillies RJ. Why do cancers have high aerobic glycolysis? Nat Rev Cancer 2004;4:891-9.
66. Webb BA, Chimenti M, Jacobson MP, Barber DL. Dysregulated pH: a perfect storm for cancer progression. Nat Rev Cancer 2011;11:671-7.
67. Kitamura I, Kochi M, Matsumoto Y, Ueoka R, Kuratsu J, Ushio Y. Intrathecal chemotherapy with 1,3-bis(2-chloroethyl)-1-nitrosourea encapsulated into hybrid liposomes for meningeal gliomatosis: an experimental study. Cancer Res 1996;56:3986-92.
68. Chen PY, Liu HL, Hua MY, Yang HW, Huang CY, Chu PC, *et al.* Novel magnetic/ultrasound focusing system enhances nanoparticle drug delivery for glioma treatment. Neurol Oncol 2010;12:1050-60.
69. Tapeinos C, Battaglini M, Ciofani G. Advances in the design of solid lipid nanoparticles and nanostructured lipid carriers for targeting brain diseases. J Controlled Release 2017;264:306-32.
70. Zhang F, Xu CL, Liu CM. Drug delivery strategies to enhance the permeability of the blood-brain barrier for treatment of glioma. Drug Des Dev Ther 2015;9:2089-100.
71. Bhujbal SV, de Vos P, Niclo SP. Drug and cell encapsulation: alternative delivery options for the treatment of malignant brain tumors. Adv Drug Delivery Rev 2014;67-68:142-53.